NURETH14-478

MODELLING AND VALIDATION OF TURBULENT BOILING FLOW IN A RECTANGULAR CHANNEL

B. Končar¹, M. Matkovič¹, A. Prošek¹

Jožef Stefan Institute

Jamova 39, SI-1000 Ljubljana, Slovenia

Bostjan.Koncar@ijs.si, Marko.Matkovic@guest.arnes.si

Abstract

The boiling flow experiments in a rectangular vertical channel, performed at the Texas A&M University, were used to validate the prediction capabilities of the NEPTUNE_CFD code. The refrigerant HFE-301 was used as a working fluid. Liquid velocity and turbulent kinetic energy profiles close to the heated wall were compared. NEPTUNE_CFD simulations successfully predict the main experimental tendencies associated with the heat flux and Reynolds number variation. However, a disagreement in velocity and turbulence magnitude can be observed in the boiling region at lower Reynolds numbers. The size of experimental bubble diameter in the vicinity of the heated wall is assessed by the means of non-dimensional analysis.

Introduction

The work presented in this paper is related to the collaborative project of the 7th European framework program NURISP (NUclear Reactor Integrated Simulation Project). One of the goals of this large-scale project is also to validate and improve the simulation capability of the three-dimensional two-fluid codes for prediction of local boiling flow processes up to DNB (Departure from Nucleate Boiling). Boiling bubbly flow in the heated vertical channel is influenced by nucleation mechanisms on the heated wall and is further influenced by the core-flow processes, such as liquid turbulence, bubble interactions and condensation in the subcooled liquid flow. For computational predictions of realistic bubbly flows, the use of averaged two-fluid approach is the best available choice. Micro-scale phenomena in the 3D two-fluid code need to be modelled by inclusion of closure models. Precise and reliable experimental data on velocity profiles, turbulence fluctuation, void fraction and bubble size within the boiling boundary layer plays a key role in better understanding of subcooled flow boiling phenomenon. Such measurements are of paramount importance to development and correct implementation of two-fluid numerical models, which are used for prediction of dominant flow boiling mechanisms in different flow regimes and for different fluids.

In this context boiling flow experiments inside a vertical square channel with one heated wall carried out at Texas A&M University (TAMU) [1] were used to validate the prediction capability of the two-fluid modelling approach. Particle Tracking Velocimetry (PTV) technique was used to measure time-averaged velocities, turbulence intensities and Reynolds stresses very close to the heated wall. These experimental data are particularly useful for assessing the two-fluid turbulence models near the heated wall. For calculation purposes the NEPTUNE_CFD code was used [2]. The program NEPTUNE_CFD is a two-fluid 3D code specifically designed for simulation of transients

in nuclear power plants. The ability of the code to predict the velocity and turbulence profiles at boiling in rectangular channel is addressed in the paper. As the measurements of void fraction and bubble sizes are not available, the bubble departure size for the considered Texas A&M experiments was assessed on the basis of existing experimental database and non-dimensional analysis.

1. TAMU experiments

A test facility at Texas A&M University was designed to investigate the subcooled boiling flow of refrigerant HFE-301 [3] at low system pressure. The refrigerant is pumped through a vertical, rectangular 530 mm long channel made of transparent polycarbonate, with 8.7 x7.6 mm nearly square cross-sectional area. A thin heater with a length of 175 mm and width of 7 mm was attached 320 mm from the channel inlet to one of the lateral walls of the channel. Figure 1 shows the schematics and dimensions of the test section. The channel cross-section has width to height ratio close to unity (w/H ~1) and a hydraulic diameter of 8.2 mm, which is typical for the fuel subchannels in boiling water reactors (BWR).

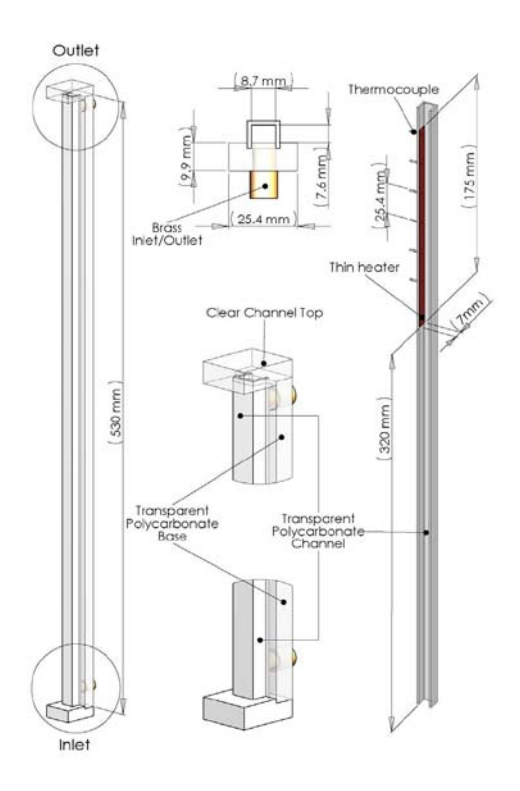


Figure 1 Schematic of the test section with dimensions [1].

The measurement plane was located 455 mm from the channel inlet to obtain fully developed turbulent flow. Flow measurements at the selected site were performed by the means of Particle Tracking Velocimetry (PTV) technique. Time-averaged and instant velocities, turbulence intensities and Reynolds stresses in axial and normal direction were measured. The data were obtained at three different Reynolds numbers 3309, 9926 and 16549. For each Re number 13 different heat fluxes were used, ranging from 0 to 64 kW/m². A constant inlet temperature of 25.5 °C was imposed for all measured cases. Detailed description of mesurment technique and procedure is given in [1]. These measurements contribute to the existing database of boiling flow measurements that can be used for validation and testing of three-dimensional multiphase models [4]. An important advantage of

considered experimental data is that they provide useful information on flow behaviour close to the wall including experimentally determined shear velocity. The information on void fraction and bubble dynamics such as bubble departure diameter, bubble frequency or bubble velocity can be acquired using the shadowgraph technique, which is envisaged for upcoming experiments. One of the weaknesses is also incomplete database on fluid properties. The fluid HFE-301 is a relatively new fluid therefore some fluid properties of the gaseous phase are not provided by the manufacturer.

2. Modelling approach

The calculations of TAMU boiling experiments are performed with the NEPTUNE_CFD code [3] and compared to experimental data. The NEPTUNE_CFD is a three-dimensional computational program based on six-equation two-fluid model and was developed especially for solving two-phase flow transients in nuclear reactor systems. A brief description of two-fluid approach and NEPTUNE_CFD models used for boiling flow simulations is given.

In boiling flow the liquid phase is treated as a continuous and the vapour bubbles are modelled as a dispersed phase. The turbulence in liquid was modelled by standard k-ɛ model. The effect of bubble wakes on the liquid turbulence is taken into account by additional terms in k-ɛ transport equations. The interfacial transfer of momentum is modelled by interfacial forces per unit volume, which include drag force, added mass force and the non-drag forces (lift, turbulent dispersion force). The interfacial heat and mass transfer due to condensation in the subcooled bulk flow was modelled by Grenoble correlation, described in the NEPTUNE_CFD manual [3]. The interfacial area concentration (interface area per unit volume) is modelled in a simplified manner by adopting a homogeneous distribution of bubble size in the flow domain. According to experimental observation by Estrada-Perez and Hassan [1] an approximate value of 1.5 mm was used for bubble diameter over the entire flow domain.

2.1 Wall boiling model

The heat transfer between the heated wall and the fluid at flow boiling is taken into account by the wall boiling model. A two-step approach is used in the NEPTUNE_CFD code. The two steps include calculation of the condition for boiling incipience in terms of critical wall superheat [3] and calculation of heat flux partitioning. By adopting the approach of Kurul and Podowski [5], the wall heat flux is split into three components:

$$\Phi_{w} = \Phi_{C1} + \Phi_{Q} + \Phi_{E} \tag{1}$$

where Φ_{Cl} denotes the single-phase convection heat flux to the liquid, Φ_Q denotes quenching heat flux that transfers cold liquid from the bulk flow to the wall periodically and Φ_E is the heat flux component needed to generate vapor bubbles. Heat flux components are calculated as follows:

$$\Phi_{C1} = A_C h_{\log} \left(T_w - T_{\delta} \right) \tag{2}$$

$$\Phi_{Q} = A_{Q} t_{Q} f \frac{2\lambda_{1} (T_{w} - T_{\delta})}{\sqrt{\pi a_{l} \tau_{Q}}}, \tag{3}$$

$$\Phi_E = \frac{\pi d_d^3}{6} f \rho_g N_a h_{\rm lg} \,. \tag{4}$$

The wall surface area per unit volume is split into two parts: an area influenced by nucleating bubbles A_Q and a "single-phase convection" area A_C unaffected by the bubbles. They are related by expression $A_Q + A_C = 1$. Parameter h_{log} in Eq. (2) denotes heat transfer coefficient in thermal boundary layer:

$$h_{\log} = \rho_l C_{pl} \frac{u^*}{T^+}, \tag{5}$$

where u^* is the wall friction velocity and T^* is the non-dimensional liquid temperature. The velocity u^* is calculated from the logarithmic law of the wall written for the liquid velocity in the wall boundary layer. The non-dimensional temperature follows a similar logarithmic profile. Other variables in equations (2) to (4) are the following: τ_Q is the quenching period between the bubble departure and beginning of the growth of a subsequent one, f is bubble departure frequency, λ_1 is liquid thermal conductivity, a_l is the liquid thermal diffusivity, D_d is maximum bubble diameter at departure, N_a is density of active nucleation sites and h_{lg} is latent heat for evaporation. The correlations used to calculate these parameters are described in the NEPTUNE_CFD manual [3]. To calculate bubble departure diameter D_d , the Unal correlation [6] is used as a base model. The correlation is described in many papers as well as in the code manual [3], therefore its description will not be repeated here.

2.2 Numerical setup

The considered computational domain of the TAMU experiment is a rectangular channel with a single heated surface, where wall boiling occurs. Due to the 3D phenomena (one side heating, swirls in the channel corners) a 2D approximation of the flow is not acceptable. Hence, a full 3D numerical domain was used with the medium grid refinement 20x20x370 in x,y,z directions, respectively. Grid refinement analysis was already performed elsewhere [7]. The length of the numerical domain was 0.53 m with the 0.32 m long unheated inlet part. Downstream of the inlet part of the channel, one side of the domain was heated in the length of 0.175 m. For the liquid velocity, a standard single-phase log law was used at the walls, whereas for the vapour velocity, a zero flux condition on the relative velocity ($dv_r/dn = 0$) was taken. A constant heat flux boundary condition was applied at the heated surface. All other wall surfaces were modelled as adiabatic boundary condition. At the inlet, a constant mass flow rate in accordance with the experimental Reynolds number and a constant temperature of 25.5 °C are set. An ambient pressure boundary condition is applied at the channel outlet. Where not specified differently all walls were considered technically smooth. The lateral distributions of various variables were measured and calculated at the location 0.455 m from the channel inlet. The simulations are carried out with the 1.0.7 version of the NEPTUNE_CFD code.

3. Results and discussion

The NEPTUNE_CFD results using the model settings as described in the previous section are presented. Where available, the predictions are compared with experimental data. Figure 2 shows temporal development of liquid velocity and void fraction for the near-wall and central cell at the axial location 0.455 m, for the medium Re and medium heat flux value. The results show that both variables converge towards finite values. The time step used for the majority of TAMU runs was

between 10^{-3} and 10^{-4} sec, except for the low Re number cases, where the smallest time step 10^{-5} sec has to be used to reach the converged solution.

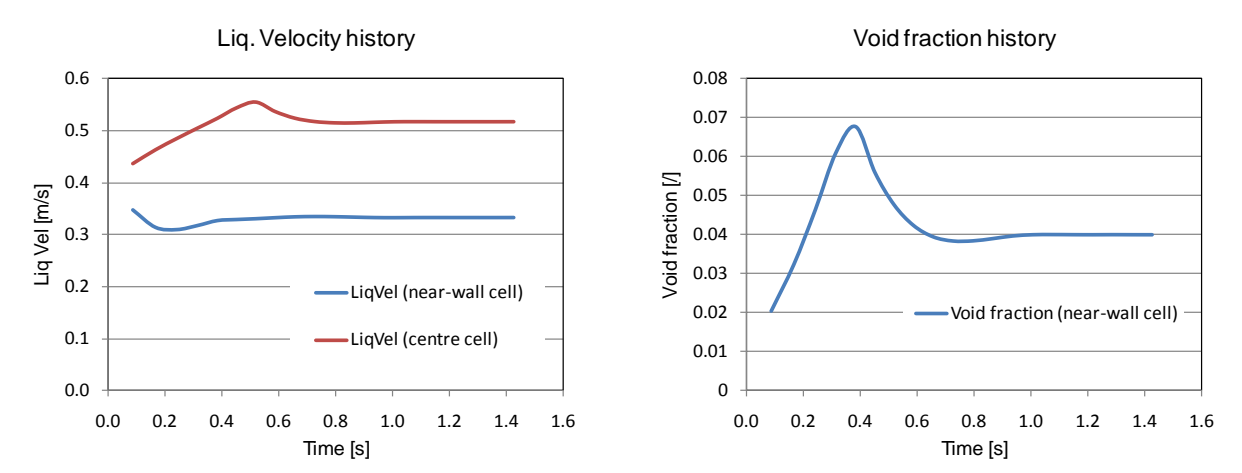


Figure 2 Time history for liquid velocity and void fraction in the NEPTUNE_CFD calculation (Re= 9926, $q_w=42.3$ kW/m²).

3.1 Velocity profiles

Comparison of liquid and vapour velocity profiles is presented in Figure 3. Experimental results are available for liquid velocity only. The results for three different Re numbers and three different heat fluxes are presented. Experimental data in the figures are denoted by symbols and simulations by lines. The same colour of symbols and lines indicates the same heat flux value. As shown, the simulations successfully predict the main experimental tendencies of velocity profile evolution. The velocity in the near-wall region increases with the increased heat flux, accompanied by the decreased axial velocity in the regions towards the unheated side of the channel.

The velocity peak near the wall is the most pronounced for the low Re number (Re= 3309). The simulations follow the experiments very well for lower heat fluxes, whereas the disagreement increased for the highest heat flux; the calculated velocity is under-predicted in the boiling region and over-predicted in the single-phase region. Another important discrepancy between the experiment and calculation can be noted. Namely, at the higher heat fluxes a shift of the maximum velocity away from the heated wall can be observed in the experiment, but it is not predicted by simulation. In the simulation the maximum velocity can always be found just near the wall. The possible reasons for not capturing the right trend could be the use of single-phase near wall boundary and inability to correctly model the boiling- induced turbulence in the near-wall region. Similar trends can be seen at the medium Re number (Re= 9926), but to a lower extent than at low Re number. The difference between liquid velocity profiles at different heat fluxes is almost negligible at the highest Re number (Re= 16549) for both measured and calculated data. The experimental and calculation data are close to each other and resemble the isothermal velocity profile since velocity increase near the heated wall is not present. This indicates that the boiling is rather suppressed at the highest Re number due to the increased mass flow rate.

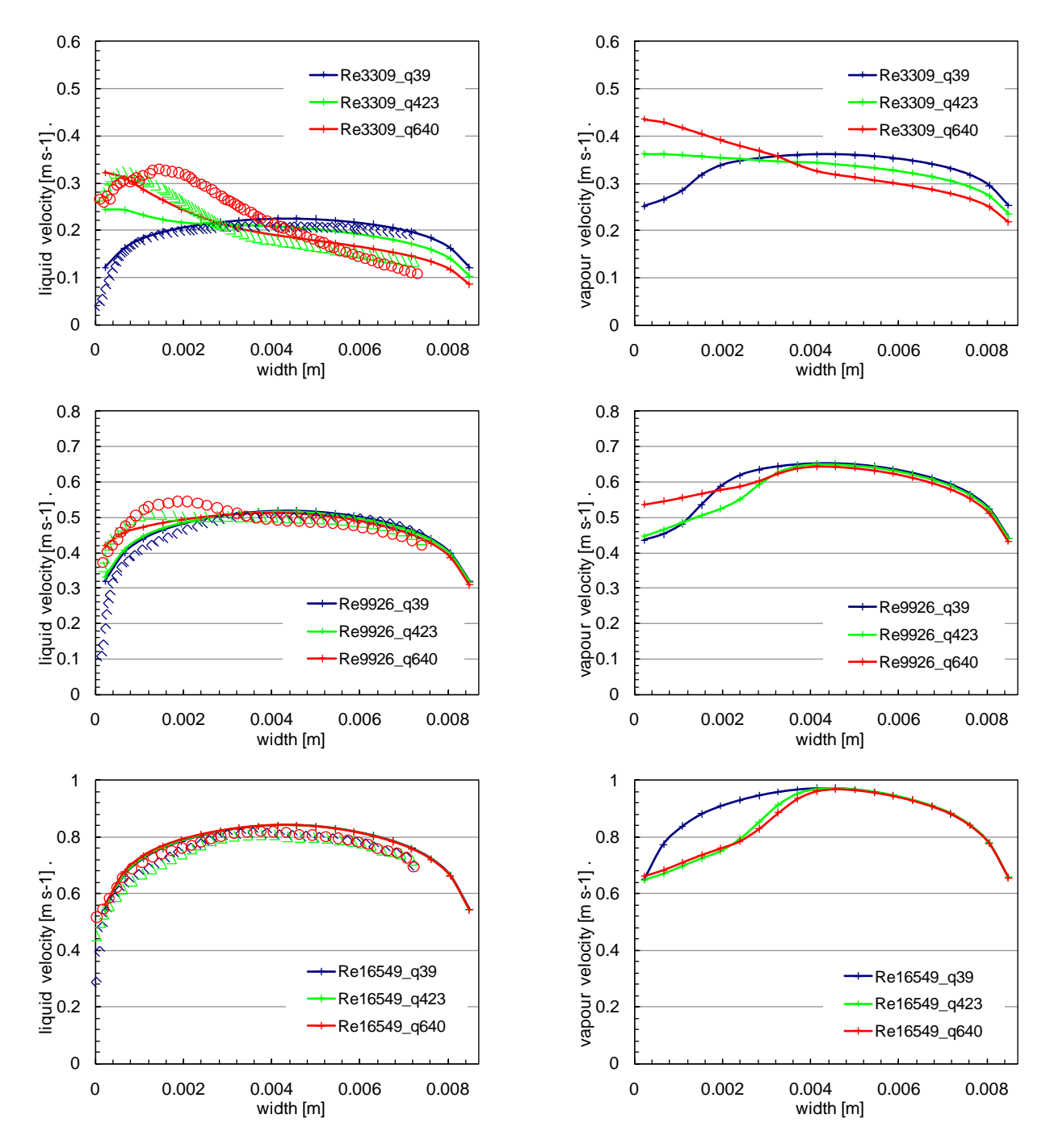


Figure 3 Liquid velocity (left) and vapour velocity (right) profiles at the measuring plane.

3.2 Turbulence

In experiments, the information on flow turbulence is provided by the measured fluctuations of velocity components. One should note that the test facility was arranged to measure instantaneous velocity fields in one plane only. Therefore, the velocity fluctuations are provided in the axial direction u' and in the direction normal to the heated surface, v'. Measured fluctuations for the highest heat flux at the lowest Re number are presented in Figure 4. This is the case with the highest boiling activity. As shown, axial velocity fluctuations are significantly enhanced in the boiling region near the heated wall.

Obviously the lateral fluctuations are much less affected by the boiling process and remain well below the axial fluctuation values over the entire channel width.

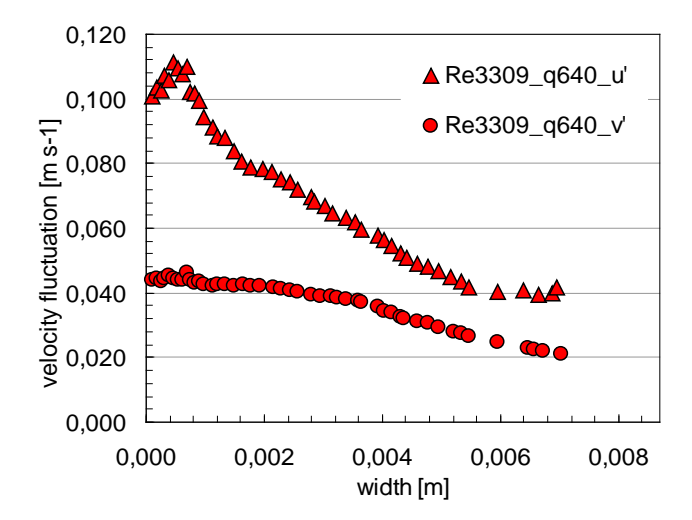


Figure 4 Experimental measurements of axial and lateral velocity fluctuations versus the distance from the wall.

Since the velocity fluctuations in the channel depth were not measured, they are assumed to have the same values as the fluctuations in the normal direction to the heated surface. Hence, the cumulative experimental turbulent kinetic energy is estimated as:

$$k_{\rm exp} = \frac{1}{2} \cdot \left(u'^2 + 2 \cdot v'^2 \right). \tag{6}$$

Comparison of calculated and experimental turbulent kinetic energy for various heat fluxes and Reynolds numbers is presented on the left side of Figure 5. The calculated void fraction profiles are presented on the right side of Figure 5 for the respective test cases. Though the experimental values of void fraction profiles are not available, the calculated void fraction should help us to at least estimate the effect of bubble-induced turbulence on the turbulent kinetic energy of the liquid.

The experimental results for low Re number (Re=3309) show drastic enhancement of k with the increased heat flux. The increase of experimental k is the largest in the boiling region near the heater, most likely due to the effect of wakes behind the bubble (the so-called bubble induced turbulence). The prevalent effect of the boiling boundary layer on the turbulence persists also at medium Re number (Re=9926). The difference in k profiles for different heat fluxes is much smaller at the highest Re number (Re=16549). Here, the high mass flow rate impedes the boiling activity and the effect of shear induced turbulence prevails. The effect of increased heat flux on the k and axial velocity profiles can be considered as minor. The comparison of experimental values of k at low heat flux values (blue symbols) indicates the increase of shear-induced turbulence with increased Re number. It may be assumed that the boiling activity here is negligible. This is supported also by the simulation results, which predict practically zero void fraction for all low heat flux cases.

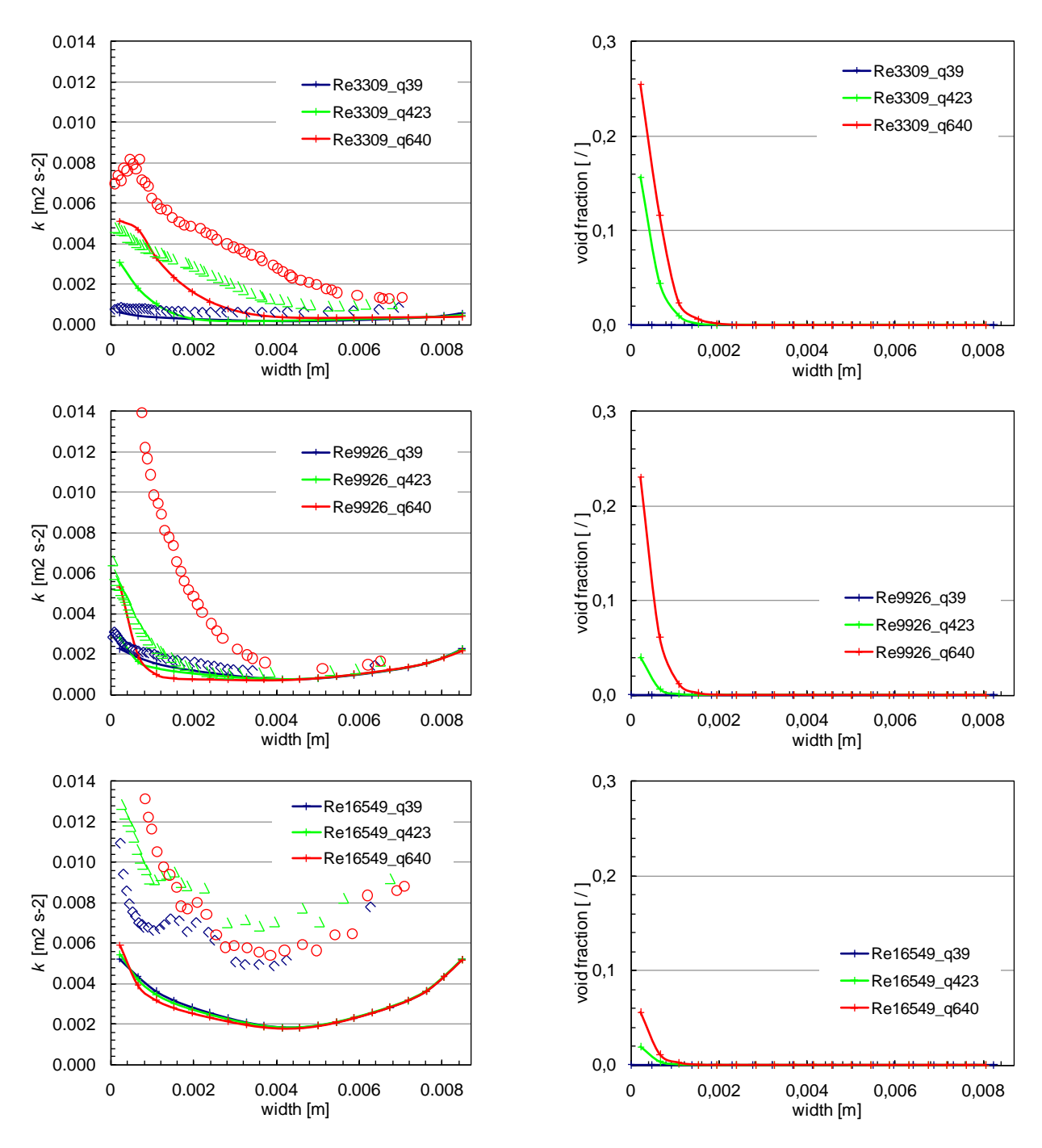


Figure 5 Turbulent kinetic energy (left) and void fraction (right) profiles at the measuring plane

The calculated profiles of turbulent kinetic energy under-predict the experimental values for most of the cases. Exceptions are the two cases at the lowest heat flux (q_w = 3.9 kW/m²) at the low and medium Re numbers, where a very good agreement can be observed. Here, the profiles of turbulent kinetic energy k and axial velocity are similar to the isothermal flow. For all other cases a significant disagreement occurs in the boiling region near the heated wall. It seems that at low and medium Re number the increase of k is closely connected to the increase of bubble-induced turbulence. The calculated k increases with the heat flux in the region near the heated wall. However the peak value and

the width of the predicted k profile are much lower and narrower as the experimental one. Although the void fraction distribution was not measured, it is very likely that the lower k values in the boiling region resulted from under-predicted void fraction. Interdependence between the bubble-induced turbulence and the void fraction profile was reported also in other experiments [8],[9] and in our previous studies [11]. At the highest Re number the k is highly under-predicted over the entire channel cross-section. However the calculations show similar trend as the experiment; the increase of k with the heat flux is almost negligible. Nevertheless, for all calculated cases the simulations follow the experimental trend: the heat flux increase results in enhanced turbulent kinetic energy near the heated wall, whereas the increased mass flow rate (Re number) causes increased k over the entire channel cross-section.

3.3 Estimation of bubble departure diameter

Simulation of boiling flow is a very demanding task that requires accurate modelling and experimental investigation of micro-scale phenomena. Due to the model limitations and lack of two-phase experimental data, our numerical model uses several assumptions and simplifications, such as constant bubble diameter in the bulk flow, simplified model of non-drag forces, single-phase wall boundary condition, etc. Different mechanisms are governing the heat transfer and vapour formation during the flow boiling process. Bubble departure diameter, nucleation site density and detachment frequency are almost directly connected to the amount of vapour formation on the heated wall. Accurate modelling of these parameters is therefore of paramount importance for void fraction prediction. Models used in current numerical simulations presented in this work require bubble departure diameter as an input parameter. Because there was no experimental data available for the modelled TAMU test runs, the bubble departure diameter was correlated from the set of other available measurements.

To evaluate the bubble departure size in TAMU tests, the database of existing experiments with measured or estimated values of bubble size near the wall can be used. The experimental database has to be supplemented by the simulation results. For the purpose of this study, we have used experimental database (see Table 1) consisting of various experiments performed with different working fluids at various operating conditions and channel geometries: DEBORA [9],[10], ASU [8] and KAERI [12]. When comparing different fluids at different operating conditions, the mechanisms controlling the boiling process may differ substantially and thus cannot be compared directly, therefore a dimensionless analysis is used. In this case, the dimensionless study is limited to Weber and Bond numbers depicting inertia, surface tension and buoyancy forces with additional density ratio term ρ_1/ρ_ν . Weber (We) and Bond (Bo) numbers are given as follows:

$$We = \frac{G^2 L}{\rho_l \sigma} \,, \tag{7}$$

$$Bo = \frac{g(\rho_l - \rho_v)L^2}{\sigma},\tag{8}$$

where G is the mass flow per unit area, L is the characteristic length scale, σ is the surface tension and ρ_l and ρ_v are densities of the liquid and vapour. To adequately predict the bubble departure diameter over the wide range of fluids and operating conditions, a new dimensionless group is used (see abscissa in Figure 6):

$$\frac{\left(\rho_{l}/\rho_{v}\right)^{0.56}}{\log(Bo \cdot We)}.\tag{9}$$

Here inertia and buoyancy forces are acting against the surface tension force while their influence is being somehow related to the thickness of the boundary layer. In fact, the thinner the boundary layer (the bigger the shear stress) the smaller is the absolute impact on bubble diameter at departure. Besides Weber and Bond numbers, in Eq. (9) the density ratio ρ_l/ρ_v is also used to involve those mechanisms in bubble departure diameter prediction. The sole purpose of the new dimensionless group is helping to estimate the input parameter (bubble departure diameter) for the selected test runs for further numerical studies in the near wall region. However, this study has no intention to propose a generic correlation for bubble departure calculation during flow boiling. Hence, the impact of different mechanisms including contact angle on bubble departure has not been taken into account neither has bubble departure been distinguished from the bubble lift-off diameter.

Considering the linear regression of measured bubble diameters in the vicinity of the heated wall taken from different experiments in Table 1, we were able to roughly estimate the bubble departure diameters for the TAMU experiments. As can be observed on the left side of Figure 6, the expected diameters for the fluid HFE 301 and the considered test conditions are ranging between 1 and 1.5 mm. The calculated bubble departure diameter values are shown on the right side of Figure 6. Two different models are compared against the each other and experiments. The Unal model [6] is used as a standard model in the NEPTUNE_CFD code. Another model proposed by Tolubinski and Kostanchuk [13] is defined as:

$$D_d = \min\left(1.4[mm], 0.6[mm] \cdot \exp\left(-\frac{\Delta T_{sub}}{45[K]}\right)\right). \tag{10}$$

The model was derived from the high-pressure water boiling experimental data with the upper limit for the bubble departure diameter, $D_d = 1.4$ mm. The correlation includes three adjustable parameters and depends solely on the local liquid subcooling. As can be seen from Figure 6, the Tolubinski model is rather insensitive to the fluid properties and remains almost constant over the entire range of parameters. Unal correlation seems to behave somewhat better as it takes into account different fluid properties and operating conditins, but it still underpredicts the experimental data. The correlation is very sensitive to the material for the boiling surface in terms of appropriate selection of the specific heat capacity, density and thermal conductivity. Nevertheless, correlation will give underestimated bubble departure diameters when the wall superheat is smaller than minimal required superheat for bubble incipience (Figure 6 right).

Table 1 Database of experiments (TAMU [1], ASU [8], DEBORA [9], KAERI [12]) and model predictions

	$ ho_{_l}/ ho_{_v}$	We	Bo	D _d [m]		
				Exp.	Tolubinski and Kostanchuk (1970)	Unal (1976)
TAMU (HFE 301)	165.6	from 26.6 to 429.5	71.1	/	4.82E-04	from 2.95E-05 to 8.47E-04
ASU (R113)	75.9	from 455.7 to 868.2	619.9	0.0007*	from 2.59E-04 to 3.06E-04	from 2.23E-04 to 3.48E-04
DEBORA (R12)	from 4.5 to 14.0	from 17383.4 to 41602.9	from 1704.1 to 2367.8	from 2.50E-04 to 7.00E-04	from 1.27E-04 to 4.01E-04	from 2.40E-05 to 6.32E-05
KAERI (Water)	1623.9	From 74.5 to 169.0	54.6	from 2.63E-03 to 2.93E-03	From 4.20E-04 to 5.44E-04	from 4.41E-04 to 1.27E-03

^{*} measured for one experiment only

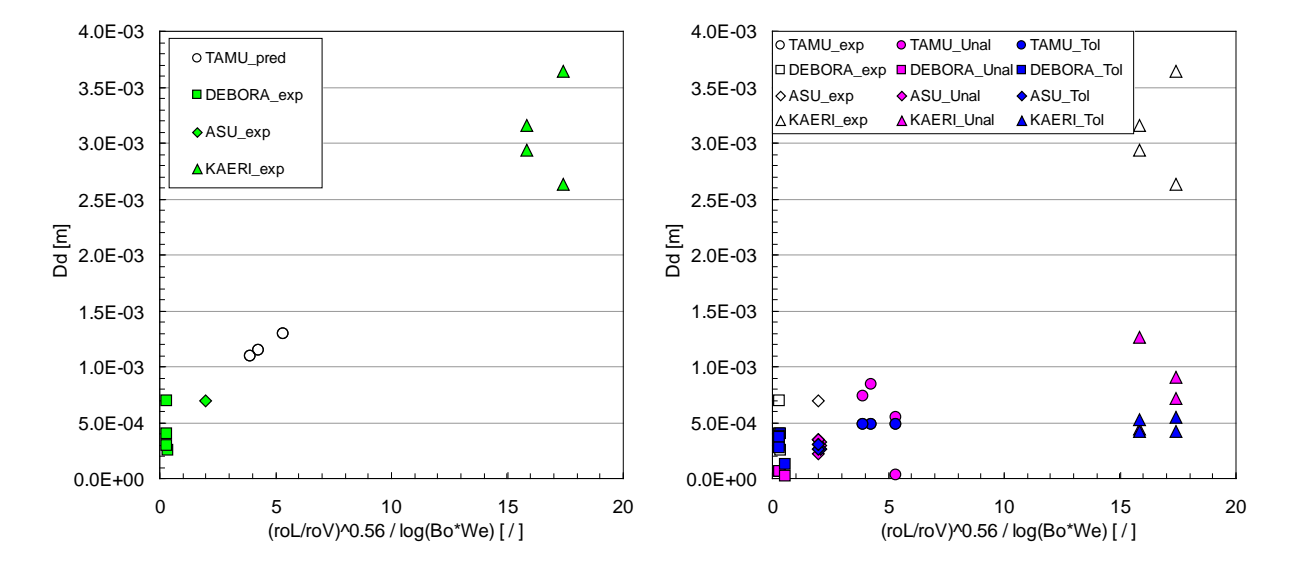


Figure 6 Measured bubble departure diameter (left) and calculated bubble departure diameter using different correlations (right).

4. Conclusions

The boiling flow experiments in rectangular vertical channel, performed at the Texas A&M University, were used to validate the prediction capabilities of the two-fluid model. The refrigerant HFE-301 was used as a working fluid. An important advantage of considered experimental data is that they provide measurements of liquid velocity and turbulence fluctuations close to the heated wall. The NEPTUNE_CFD computer code with the standard set of modelling parameters was used to simulate the experimental data. Axial velocity and turbulent kinetic energy profiles were compared. Simulations succeed to predict the main experimental tendencies associated with the heat flux and Reynolds number variation. Nevertheless, an under-prediction of velocity in the boiling region accompanied by significant under-prediction of turbulence may be observed. To estimate the size of bubble departure diameter for TAMU experiments, the database of existing experiments with

different fluids and operating conditions was used and correlated in terms of relevant nondimensional numbers.

5. Acknowledgements

This work was financially supported in part by the Slovenian Research Agency and partly through the NURISP integral project (7th Euratom Framework Program).

6. References

- [1] C.E. Estrada-Perez and Y.A. Hassan, 2010, PTV experiments of subcooled boiling flow through a vertical rectangular channel, *Int. J. Multiphase Flow*, Vol. 36, Issue 9, pp. 691-706.
- [2] Lavieville, J., Quemerais, E., Mimouni, S., Boucker, M., Mechitoua, N., 2005. NEPTUNE CFD V1.0 Theory Manual.
- [3] HFE-301 3M, Product information, 3M Novec 7000, engineered fluid, 2009, website: http://multimedia.mmm.com/mws/
- [4] D. Bestion, D. Caraghiaur, H. Anglart, P. Péturaud, E. Krepper, H.M. Prasser, D. Lucas, M. Andreani, B. Smith, D. Mazzini, F. Moretti, J. Macek, "Deliverable D2.2.1: Review of the Existing Data Basis for the Validation of Models for CHF", NURESIM-SP2-TH D2.2.1., 2006.
- [5] Kurul N., Podowski M.Z., 1990. Multidimensional effects in forced convection subcooled boiling. Proceedings of the Ninth International Heat Transfer Conference, Jerusalem, Israel, August 1990, 21-26.
- [6] Unal H.C., 1976, Maximum bubble diameter, maximum bubble -growth time and bubble -growth rate during the subcooled nucleate flow boiling, Int. J. Heat Mass Transfer 19, pp. 643-649.
- [7] Marko Matkovič, Boštjan Končar, Ivo Kljenak, Carlos E. Estrada-Perez, Yassin A. Hassan, 2011, CFD Simulation of Boiling Flow Experiment in a Rectangular Vertical Channel, Proceedings of ICONE19 19th International Conference on Nuclear Engineering, May 16-19, 2011, Chiba, Japan.
- [8] R. P. Roy, S. Kang, J. A. Zarate, A. Laporta, 2002, Turbulent Subcooled Boiling Flow— Experiments and Simulations, *J. Heat Transfer*, Vol 124, pp. 73-93
- [9] Christophe Morel, Wei Yao, Dominique Bestion, 2003, Three Dimensional Modeling of Boiling Flow for the Neptune Code, 10th International Topical Meeting on Nuclear Reactor Thermal Hydraulics (NURETH-10), Seoul, Korea, October 5-9, 2003.
- [10] Garnier, J., François, F., DEBORA data bank (CD), 2006.
- [11] B. Končar, E. Krepper, 2008,CFD simulation of convective flow boiling of refrigerant in a vertical annulus, Nucl. Eng. Des. 238, pp. 693-706.
- [12] T.H. Lee, G.C. Park, D.J. Lee, 2002, Local flow characteristics of subcooled boiling flow of water in a vertical concentric annulus, *Int. J. Multiphase Flow*, Vol. 28, pp. 1351–1368
- [13] Tolubinski V.I., Kostanchuk D.M., 1970, Vapour bubbles growth rate and heat transferintensity at subcooled water boiling, 4th Int. Heat Transfer Conf., Vol. 5, paper No. B-2.8, Paris.